ORIGINAL PAPER

RJME Romanian Journal of Morphology & Embryology http://www.rjme.ro/

Zinc–Boron–PLGA biocomposite material: preparation, structural characterization, and *in vitro* assessment

MARIA VIORICA CIOCÎLTEU[1,2], ION ROMULUS SCOREI[1)], GABRIELA RĂU[1,3)], CLAUDIU NICOLICESCU[4)], ANDREI BIŢĂ[1,5)], VLADIMIR LUCIAN ENE[6)], ANDREEA SIMIONESCU[7)], ADINA TURCU-ŞTIOLICĂ[8)], VENERA CRISTINA DINESCU[9)], JOHNY NEAMŢU[1,10)], LAURENŢIU MOGOANTĂ[11,12)], GEORGE DAN MOGOŞANU[1,5)]

[1)]*Department of Biochemistry, BioBoron Research Institute, S.C. Natural Research S.R.L., Podari, Dolj County, Romania*

[2)]*Department of Analytical Chemistry, Faculty of Pharmacy, University of Medicine and Pharmacy of Craiova, Romania*

[3)]*Department of Organic Chemistry, Faculty of Pharmacy, University of Medicine and Pharmacy of Craiova, Romania*

[4)]*Department of Engineering and Management of Technological Systems, Faculty of Mechanics, University of Craiova, Drobeta Turnu-Severin, Romania*

[5)]*Department of Pharmacognosy & Phytotherapy, Faculty of Pharmacy, University of Medicine and Pharmacy of Craiova, Romania*

[6)]*Department of Science and Engineering of Oxide Materials and Nanomaterials, Faculty of Chemical Engineering and Biotechnologies, National University of Science and Technology Polytechnic Bucharest, Romania*

[7)]*Department of Chemistry, Faculty of Exact Sciences, University of Craiova, Romania*

[8)]*Department of Pharmacoeconomics, Faculty of Pharmacy, University of Medicine and Pharmacy of Craiova, Romania*

[9)]*Department of Health Promotion and Occupational Medicine, Faculty of Medicine, University of Medicine and Pharmacy of Craiova, Romania*

[10)]*Department of Physics, Faculty of Pharmacy, University of Medicine and Pharmacy of Craiova, Romania*

[11)]*Research Center for Microscopic Morphology and Immunology, University of Medicine and Pharmacy of Craiova, Romania*

[12)]*Romanian Academy of Medical Sciences, Craiova Subsidiary, Romania*

Abstract

Nowadays, the state-of-the-art discoveries in the field of delivery systems for therapeutic purposes have redefined the importance of biocompatible and biodegradable poly(lactic-*co*-glycolic acid (PLGA) nanocomposites. The study aimed to obtain a biocomposite material, with improved properties of its constituents [zinc–boron (Zn–B) complex and PLGA], by a simple, cost-effective method. The water/oil/water double emulsion technique allowed the adjustment of the synthesis parameters, to maximize the degree of Zn–B complex encapsulation. The morphological aspects of the samples were established by scanning electron microscopy (SEM). Particle size distribution was determined by dynamic light scattering (DLS). Morphology was typical for PLGA, spherical one. Depending on the synthesis conditions, the obtained particles have diameters between 10–450 nm. *Zeta* potential (ZP) showed that the particles have electronegative surface charge, offering a favorable perspective on aggregation, flocculation, and dispersion phenomena. It was observed, applying the design of experiments, that the particles size increased with increasing amounts of PLGA and polyvinyl alcohol (PVA), while ZP increased with higher PLGA and smaller PVA amounts in the formulation. The encapsulation efficiency was determined by ultra-high performance liquid chromatography/mass spectrometry (UHPLC/MS). The *in vitro* assessment was performed using Vero CCL-81 epithelial cell line and the 3-(4,5-Dimethylthiazol-2-yl)-2,5-diphenyltetrazolium bromide (MTT) test. Zn–B–PLGA biocomposite has promising characteristics and can be used for future biomedical applications.

Keywords: Zn–B–PLGA biocomposite, design of experiment, scanning electron microscopy, dynamic light scattering, ultra-high performance liquid chromatography/mass spectrometry, *in vitro* assessment.

Introduction

Poly(lactic-*co*-glycolic acid) (PLGA) has a series of properties (adjustable sizes, stability, biodegradability, the possibility of surface functionalization) that offers it numerous advantages already described that led to its extensive use as a drug delivery system [1].

The flexibility of degradation is an important factor that makes PLGA suitable to produce medical devices, such as nanoparticles (NPs), implants, or grafts. PLGA consists of a class of biodegradable polymers that are approved by the *Food and Drug Administration* (FDA), which gives them sustainability in terms of drug delivery. These polymers have been studied as vehicles for proteins, peptides, ribonucleic acid (RNA) or deoxyribonucleic acid (DNA) [2].

PLGA-based microparticles (MPs) or NPs represent most formulations on the pharmaceutical market, there are 14 products with PLGA clinically approved and currently used in medical practice in diseases such as prostate cancer, osteoarthritis, diabetes, etc., and many other PLGA-based products in clinical trials [3–6].

PLGA in living tissues

PLGA is considered compatible with living tissues, meaning it does not elicit a significant immune response or toxic effects in living tissues. It has been extensively studied and used in preclinical and clinical settings. However, it is important to note that individual responses can vary, and careful consideration of factors, such as degradation rate, molecular weight, and specific application is necessary to ensure optimal biocompatibility [1, 3–5].

In the body, PLGA undergoes a process of hydrolysis and forms lactic acid (LA) and glycolic acid (GA) [7]. These original monomers of PLGA are secondary products of metabolic pathways in the human body. The human body can metabolize GA to toxic oxalic acid, but the amounts in typical applications are negligible and systemic toxicity is minimal [8]. On the other hand, the acidic PLGA degradation medium can induce an autocatalytic environment because the local pH drops sufficiently for this to be possible. The autocatalytic capacities of PLGA are size dependent. The first surface that begins to degrade is the center of the PLGA matrix because this is where acidic oligomers accumulate. Thus, an acidic center is formed from which erosion begins [7, 8].

Polymer–drug interaction was also observed in the studies, which gives PLGA a potential degree of toxicity in drug dose delivery. At the same time, toxicity can also be associated with the inconstant release of medicinal compounds, but additional research is needed to prove this aspect [9].

Boron and Zinc as essential elements

Boron (B) is an essential element, although it is required in small amounts compared to other essential elements. It plays important roles in various biological processes and is necessary for the growth and development of plants, animals, and humans [10]. In plants, B is involved in cell wall formation, membrane integrity, carbohydrate metabolism, and the transport of nutrients [11]. It also plays a role in pollen germination and fruit development. In animals and humans, B is involved in bone health, as it influences the metabolism and utilization of calcium, magnesium, and vitamin D [12]. It also plays a role in brain function and cognitive performance [10, 11].

B has a huge impact on the microbiota, particularly in the gastrointestinal tract [13–20]. There are a few studies that suggest that it may have a modulatory role. One study published in the *Journal of Trace Elements in Medicine and Biology* investigated the influence of B on gut microbiota (GM) in rats. The results showed that B supplementation led to changes in the composition of the GM, including an increase in the abundance of certain bacterial species. Karatekeli *et al.* (2023) showed that B exhibits hepato-protective antioxidant, anti-inflammatory, and antiapoptotic effect in rats exposed to aflatoxins [14]. Arciniega-Martínez *et al.* (2022) examined the effects of B on immune function, showing that B-containing compounds induce an immune response on cells [15].

One of the most important trace elements in the human body, zinc (Zn) is essential for regulatory, structural, and catalytic activities, involving immune response, oxidative stress, homeostasis, ageing, and apoptosis [21, 22]. Zn has a critical role for immunity and cell survival, being involved in many biological functions by the fact that it is a component of more than 300 enzymes and 1000 transcription factors [23]. Zn affects GM [24], inhibits pathogenic bacteria [25], meliorate incidence of diarrhea by reducing intestinal damage and improving anti-inflammatory factors [26].

Zn–boric acid (BA) biological interplay has been evidenced in rats. At an equivalent B concentration, Zn borate exhibited low acute toxicity [median lethal dose (LD_{50}) >10 g/kg body weight (b.w.)] unlike disodium tetraborate pentahydrate (LD_{50} of 3.3 g/kg b.w.). Moreover, in a 28-day subacute oral gavage assay, no toxic effects were observed for 1 g Zn borate/kg b.w./day (equivalent to 0.05 g B/kg b.w./day) [27].

Zn–B complex: novel natural active Zn and B-based dietary supplement

In vitro and *in vivo*, Zn–B complex turned out to be a non-toxic, biocompatible, and biodegradable nutritional supplement, significantly increasing alpha$_2$-macroglobulin (A2M) levels [28, 29]. It has been shown that Zn–B complex has a similar composition to fructoboric acid, a naturally occurring compound found in plants [30].

In recent years, the use of PLGA formulations for oral controlled release has gained more and more importance [31, 32]. Subsequently, PLGA can release Zn and B into the colon, two essential elements for a healthy symbiosis between the microbiota and the human host.

Aim

The aim of the study was the preparation and structural characterization of a new biocomposite material with PLGA as a transporter of Zn–B complex for systemic administration. The preparation was carried out by a simple, cost-effective method, optimizing the key parameters for the adjusting of the Zn–B complex amount encapsulated into the PLGA sphere, as well as the biocomposite dimensions, stability, and functionality, and it was submitted as a United States Provisional Patent Application [18]. In addition, the *in vitro* assessment of Zn–B–PLGA biocomposite was performed using Vero CCL-81 epithelial cell line and the 3-(4,5-Dimethylthiazol-2-yl)-2,5-diphenyltetrazolium bromide (MTT) test.

Materials and Methods

Chemicals, reagents, and cell line

Poly(D,L-lactide-*co*-glycolide) 65:35, molecular weight (MW) 40 000–75 000, was purchased from Sigma-Aldrich (Taufkirchen, Germany). Dichloromethane (DCM), polyvinyl alcohol (PVA) 8-88 (MW approx. 67 000), ammonium acetate, potassium bromide and LiChrosolv® water and acetonitrile for chromatography were achieved from Merck Millipore (Darmstadt, Germany). For the Zn–B complex preparation, Zn powder, BA and fructose were purchased also from Merck Millipore. For *in vitro* assessment, dimethyl sulfoxide (DMSO), ethylenediaminetetraacetic acid (EDTA), Eagle's Minimal Essential Medium (EMEM), fetal bovine serum (FBS), MTT, phosphate-buffered saline (PBS), trypsin and Vero CCL-81 epithelial cell line were purchased from Sigma-Aldrich.

Preparation of Zn–B complex

Zn–B complex was synthesized based on general methods used for the synthesis of various borate complexes with carbohydrates (fructose, sorbitol, mannitol) and B inorganic anions [33–36]. The optimization of Zn–B complex synthesis was made using a Büchi-type reactor made of steel, with a capacity of 300 mL, and which can withstand a pressure of up to 100 bar, equipped with temperature probe, pressure gauge, pneumatic connection, and safety valve. For the activation of metallic Zn, 9.146 g (70 mmol) of Zn powder and 300 mL of distilled water were added to a Büchi-type reactor, equipped with two necks, device for nitrogen (N_2) admission and overpressure regulation, and with a thermometer. The air was gradually replaced, for 10–15 minutes, with inert gas (purging with N_2). The reaction mixture was heated to 140–150°C, for three hours, under strong stirring (plate with electromagnetic stirrer), to activate metallic Zn. After three hours, the reaction mixture from the metallic Zn activation was cooled to 50–60°C, then 12.412 g (68.95 mmol) of fructose and 2.137 g (34.47 mmol) of BA (in this order) were gradually added, while stirring. Next, the reaction mixture was kept under stirring for 60 minutes, at a temperature of 50–60°C. After three hours, the reaction mixture has a temperature of 91.5°C and a pH of 6.36. After another 60 minutes, the reaction mixture was filtered under vacuum to separate the excess of unreacted metallic Zn.

Preparation of Zn–B–PLGA biocomposite

W_1 aqueous phase: 50 mg of Zn–B complex were solubilized in 2 mL aqueous solution with 4% PVA 8-88 (*w/v*).

Oil phase O: 50–150 mg of PLGA 65:35 was dissolved in DCM.

The two phases were brought into contact and mixed at 45000 rpm in a Heidolph Silent Crusher Vortex (Wood Dale, Illinois, USA) to obtain the *W_1/O* primary emulsion.

W_2 aqueous phase: 95 mL of aqueous solution with 1–4% PVA 8-88 as emulsifier (*w/v*).

The primary emulsion was added dropwise to the secondary aqueous phase stirred at 1000 rpm for three hours to evaporate the DCM.

The particles were centrifuged at 11 000 rpm, washed and frozen overnight. The final suspension was subjected to a lyophilization process using an Alpha 1-2 LSCbasic freeze dryer (Martin Christ Gefriertrocknungsanlagen GmbH, Osterode am Harz, Germany), as follows: the suspended particles were frozen at -55°C overnight and at 0.02 mbar for 48 hours.

Design of experiments analysis

To solve design constraints and perform minimum experimental runs, we used design of experiments (DoE) by a systematic quality by design (QbD) approach (Table 1). The independent variables (factors) were the concentrations of PVA and of PLGA, whereas the dependent variables (responses) were the size of the Zn–B–PLGA biocomposite and the *zeta* potential (ZP). According to a full factorial (two levels) design, interaction model, we performed seven experiments (Table 2). Only terms with significance level less than $p<0.05$ were included into the experimental model. We calculated R^2 (the fraction of the variation in the response explained by the model), Q^2 (the predictive power of the models), *F*-value (the mean regression ratio), model validity (to which extent the measurement meets the real-life situations), reproducibility (the ability to achieve the same output when the input is the same).

Table 1 – ***Independent variables (factors) and their levels***

Independent variable	Symbol	Levels		
		-1	*0*	*+1*
PVA concentration [%]	X_1	1	2.5	4
PLGA concentration [mg]	X_2	50	100	150

PLGA: Poly(lactic-*co*-glycolic acid); PVA: Polyvinyl alcohol.

Table 2 – ***Experimental design matrix of responses***

Experiment	PVA concentration [%]	PLGA concentration [mg]	Particle size [nm]	ZP [mV]
N1	1	50	17.7± 0.071	-1.11± 0.55
N2	4	50	225± 0.912	-5.07± 0.57
N3	1	150	365.7± 0.05	3.45± 2.49
N4	4	150	435.2± 0.079	-2.19± 0.64
N5	2.5	100	232.9± 0.411	-3.71± 1.69
N6	2.5	100	241.9± 0.04	-3.11± 0.45
N7	2.5	100	257.5± 0.246	-2.78± 0.33

PLGA: Poly(lactic-*co*-glycolic acid); PVA: Polyvinyl alcohol; ZP: Zeta potential.

The experimental data obtained from the seven (N1–N7) experiments were fitted to a polynomial model, which allows prediction of the formulation variables on the Zn–B–PLGA biocomposite characteristics, using MODDE *ver*. 21.1 for Windows software (Sartorius Stedim Data Analytics AB, Umeå, Sweden). The mathematical approach allows each *Y* response to be represented by an equation:

$$Y = b_0 + b_1X_1 + b_2X_2 + b_{12}X_1X_2$$

where X_1 and X_2 – independent variables (as in Table 1); b_1 and b_2 – the estimation of the main effects of the X_1 and X_2 factors; b_{12} – the estimation of the interaction between X_1 and X_2 factors.

Spectral characterization

Fourier-transform infrared (FTIR) spectra were recorded on a Thermo Nicolet Avatar 370 FTIR spectrometer (Thermo Nicolet Corp., Madison, WI, USA) in potassium bromide pellets, using EZ Omnic *ver*. 7.3. software and spectral library (Thermo Electron Corp., Madison, WI, USA). The samples were scanned within the range 4000–400 cm^{-1}. Thirty-two scans were performed, with a resolution of 16 cm^{-1}.

Morphological aspects

Scanning electron microscopy (SEM) was carried out to highlight aspects related to the morphology of the samples, such as shape, agglomeration tendency, porous character. To determine the morphology and elemental composition of the obtained biocomposite, a high-resolution SEM, FEI Inspect F50 (FEI Company, Hillsboro, Oregon, USA) was

used. The microscope is equipped with a field emission gun (FEG) and an energy-dispersive X-ray spectrometer (EDS), with a resolution at MnK of 133 eV. The acquisition of micrographs was made with an energy value of 30 keV and a point-to-point resolution of 1.2 nm, at different magnifications, using the secondary electron detector.

For SEM analysis, we fixed the samples 20 minutes, at room temperature, in 4% paraformaldehyde (PFA). After three PBS washes, to dehydrate the cells, the samples were sequentially immersed in 70%, 90% and 100% ethanol, 15 minutes twice for each concentration. Then, the samples were air dried. Since the samples to be analyzed do not have electrical conductivity, their preparation was necessary, which consists of a metallization process (covering the surface to be analyzed with a film of gold NPs approx. 4 nm thick). This process of obtaining electrical conductivity takes 60 seconds. The analysis was carried out in a vacuum, by measuring the energy of the secondary electrons resulting from the interaction of the surfaces with the primary electron beam.

Dynamic light scattering analysis

The numerical and volumetric distribution of the synthesized NPs (hydrodynamic diameter) was measured by the dynamic light scattering (DLS) technique using a Brookhaven 90 Plus equipment (Brookhaven Instruments Corp., Austin, Texas, USA) provided with laser of 35 mW output power and 660 nm wavelength. The analysis of the Brownian motion of the particles brought into the liquid medium and dispersed (by ultrasonication) was correlated with the size of the particles by laser illumination and analysis of the intensity of scattered light fluctuations. The samples were diluted in water and sonicated for five minutes. The analysis was performed at 25°C, diffraction angle of 90°.

Zn–B complex loading efficiency in Zn–B–PLGA biocomposite

The loading efficiency (LE) [%] was determined by measuring 25 mg of Zn–B–PLGA biocomposite NPs in 2 mL of water. The dispersion was initially stirred under ultrasound and then left for 40 days for the complete release of the active principle and complete hydrolysis of the polymer. The obtained solution was filtered, diluted 1:20 and subjected to ultra-high performance liquid chromatography/ mass spectrometry (UHPLC/MS) analysis. Waters (Milford, Massachusetts, USA) Arc System coupled with a Waters QDa MS detector was used for the UHPLC/MS analysis. The column was a Waters Atlantis Premier BEH Z-HILIC (2.1×100 mm, 2.5 μm) eluted with two solvents: A (10% ammonium acetate in water) and B (acetonitrile) in isocratic mode (25% A). The flow rate of the mobile phase was set to 0.3 mL/min. The column temperature was equilibrated to 30°C. The injection volume was 5 μL. The QDa MS detector was set to negative mode at 0.8 kV for the capillary, 20 V for the cone voltage and 400°C for the capillary. The mass range was set at *m/z* 100–600 for spectra collection and Selected Ion Recording (SIR) mode was used for quantification at *m/z* 367 [27, 29].

LE [%] was calculated using formula:

$$\text{LE [\%]} = \frac{Mass\ of\ Zn\text{–}B\ complex\ [mg]}{Mass\ of\ Zn\text{–}B\text{–}PLGA\ [mg]} \times 100$$

Cell culture and MTT assay

The cell line and the experimental conditions are specified in a previously published paper [28], as follows: Vero CCL-81 epithelial cell line obtained from African green monkey kidney; supplementation of EMEM with 10% FBS; incubation at 37°C in a humid atmosphere of 5% carbon dioxide (CO_2); trypsin–EDTA treatment to detach adherent cells with 80% confluence; detached cells were seeded in 96-well plates (10^4 cells/cm^2 density) and allowed for 24 hours to grow in monolayer; cells were incubated for an additional 24 hours with sterile medium of Zn–B–PLGA biocomposite (0.1, 0.5, 1, 3, 5, 7 and 10 mM); 5% DMSO was used as positive control of cytotoxicity; the genuine culture plate represented the negative control of cytotoxicity [37]. The contrast phase microscopy (Olympus CKX41 microscope, video camera, image capture, CellSens software) was used for the assessment of Vero cell line density and morphology.

For the assessment of cytotoxicity, cell viability and proliferation, the MTT test was applied. MTT reagent (1 mg/mL) was added in cell culture medium 24 hours after the Zn–B–PLGA biocomposite treatment, only by applying the prior washing with PBS of the cell culture monolayer. The optical density (OD) of the metabolically viable Vero cell line, represented by the DMSO-solubilized formazan dye, a MTT reduction product, was assessed by spectrophotometry (550 nm) after three hours incubation at 37°C [38].

Statistical analysis

Mean diameter, polydispersity index (PDI), ZP and encapsulation efficiency consisted of mean values (n=5) and standard deviation (SD). The non-parametric values were analyzed using the Kruskal–Wallis test. For *in vitro* assessment, the statistical analysis was performed using the Statistical Package for the Social Sciences (SPSS) *ver*. 25.0 for Windows (SPSS, Chicago, IL, USA). Differences between cell cultures treated with Zn–B–PLGA biocomposite and control cell line were evidenced by one-way analysis of variance (ANOVA). Statistical comparisons were performed with the Student's unpaired test when data exhibit a normal distribution. Differences were considered significant for p-values less than 0.05.

Results

Optimal experimental design of Zn–B–PLGA biocomposite preparation

The water/oil/water (*W/O/W*) double emulsion method [39] is one of the most used techniques for PLGA-based biomaterials due to the simplicity of the process, the low cost of the used instrumentation, and the easiness in the parameters control [40]. The method consists in adding the insoluble volatile organic phase (DCM) [41] over the W_1 aqueous phase, which contains Zn–B complex dissolved in the aqueous phase, emulsifying at a high speed (45 000 rpm) with a homogenizer. The result is a water-in-oil primary emulsion that was added by continuous mixing to a very large amount of W_2 aqueous phase (95 mL) containing different surfactants, in our case PVA (1–4%, *w/v*), forming a *W/O/W* double emulsion. The concentration of the polymer was chosen between 50 and 150 mg. The use of DCM as

organic solvent leads to Zn–B–PLGA biocomposite spheres of 15–450 nm size (as shown by DLS), while for the use of other type of organic solvent (acrylonitrile [42], tetrahydrofuran [43]) leads to obtaining smaller particles, with diameters less than 100 nm.

To determine the levels of factors that ensure optimal size and ZP, we fitted an initial model that explained over 99% of the size's variation and over 94% of the ZP's variation, which indicates that all responses were well fitted by the experimental model. The predictive power of the model was high for size (82%) and moderate for ZP (51%), which indicates that all responses were well predicted by the experimental model. Furthermore, model validity (0.62 for size and 0.86 for ZP) and reproducibility (0.99 for size and 0.86 for ZP) values were greater than 0.6 and 0.8, respectively, suggesting a reduced experimental error. *F*-value for regression was 128.26 (p=0.001) for size and 15.9 (p=0.024) for ZP, respectively (Table 2).

According to the coefficient list for designed model, each response was represented by the equations:

$$\text{Size} = 253.7 + 69.2*X_1 + 139.55*X_2 - 34.45*X_1*X_2$$

$$\text{ZP} = -3.06 - 0.68*X_1 + 0.14*X_2 + 1.31*X_1*X_2$$

where X_1 and X_2 – independent variables; *ZP – zeta* potential.

The results of the ANOVA test showed not only the p-value was lower than 0.05 for all responses, but also p-value for the lack of fit was greater than 0.05 for all responses (F=3.12, p=0.219 for size and F=0.46, p=0.566 for ZP), which confirmed that the proposed model was adequate, reliable, with a good predictive power.

The responses contour plots illustrated the quantitative effect of the factors on the two responses, identifying the optime values for the two factors to obtain the expected responses (Figure 1).

After performing optimizer within the design space with a target of 200 nm for size and minimize for ZP, the model proposed the X_1=4% and X_2=50 mg values. Furthermore, using the prediction list outside the design space, the characteristics of the optimum formulation could be obtained for X_1=5% and X_2=10 mg values, the model predicting the size 221 nm (119 nm to 323 nm) and ZP -8.3 mV (-11 mV to -5.7 mV) values.

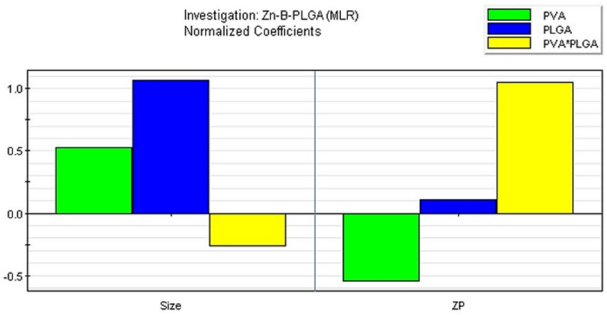

Figure 1 – ***Coefficient overview plot for both responses. B: Boron; MLR: Multiple linear regression; PLGA: Poly(lactic-co-glycolic acid); PVA: Polyvinyl alcohol; Zn: Zinc; ZP: Zeta potential.***

FTIR characterization

FTIR analysis highlighted the carbonyl (–C=O) stretching vibration that appeared as a prominent peak in the PLGA spectrum, at 1736 cm^{-1} (simple PLGA) and at 1734 cm^{-1} (Zn–B–PLGA biocomposite), respectively. The aliphatic C–H stretching vibrations can also be observed in the range of 2800–3000 cm^{-1} for the methylene ($–CH_2–$) groups of the polymer. The stretching vibration of the ester (C–O–C) bond was observed both in simple PLGA and Zn–B–PLGA biocomposite at 1255 cm^{-1} and 1251 cm^{-1}, respectively. Hydroxyl stretching vibrations in Zn–B complex due to the presence of alcohol groups appeared as a broad band in the range of 3200–3600 cm^{-1}. Carbonyl stretching vibration also appeared in the Zn–B complex at 1638 cm^{-1} due to the –C=O group of the fructose molecule. The peaks at 1060 cm^{-1} and 1065 cm^{-1} from Zn–B complex and Zn–B–PLGA biocomposite, respectively, can be attributed to the C–O–C (from etheric group) vibrations, while the peaks at 1423 cm^{-1} and 1427 cm^{-1} correspond to C–H stretching vibrations, being influenced by intra and intermolecular factors (Figure 2).

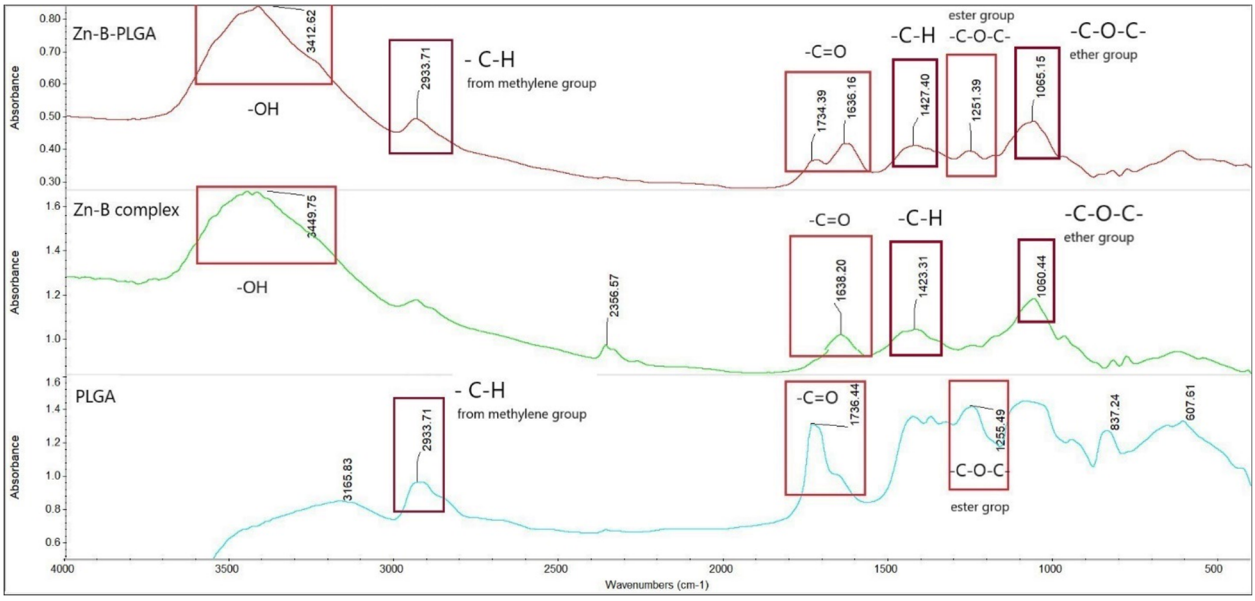

Figure 2 – ***FTIR analysis of PLGA, Zn–B complex and Zn–B–PLGA biocomposite. B: Boron; FTIR: Fourier-transform infrared; PLGA: Poly(lactic-co-glycolic acid); Zn: Zinc.***

Morphological aspects

SEM at different magnitudes revealed a porous material, the spherical shape of the NPs of Zn–B–PLGA biocomposite are well organized. The three-dimensional aspect of the lattice was also highlighted by SEM (Figure 3, A–E).

According to the energy dispersive X-ray (EDX) mapping, the predominant elements content in the Zn–B–PLGA biocomposite are C (56.33 *wt*%), O (43.46 *wt*%), Zn (0.21 *wt*%). Our EDX analyzer can detect elements with an atomic number from 11 (natrium – Na) upward, so B, our major interest element could not be detected by this method (Figure 4).

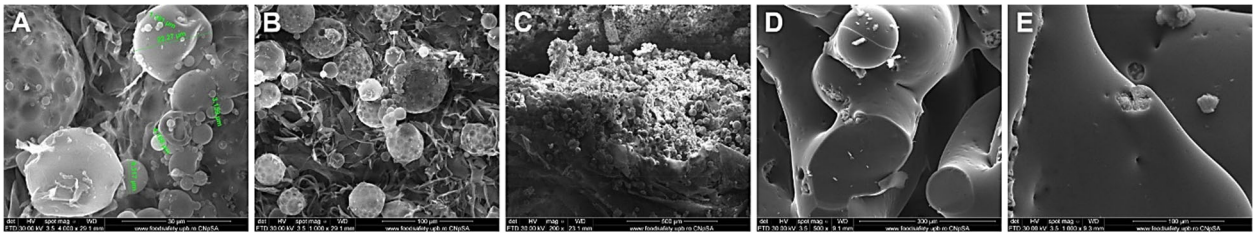

Figure 3 – ***Morphology of the Zn–B–PLGA biocomposite nanoparticles. SEM micrographs at different magnitudes: (A–C) Zn–B–PLGA biocomposite; (D and E) Zn–B complex. B: Boron; PLGA: Poly(lactic-co-glycolic acid); SEM: Scanning electron microscopy; Zn: Zinc.***

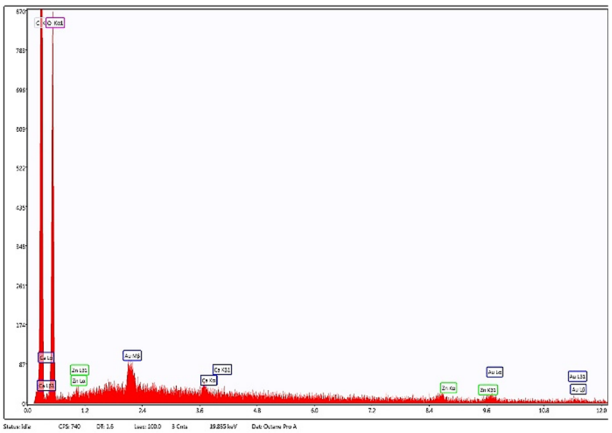

Figure 4 – ***EDX mapping analysis of Zn–B–PLGA biocomposite. B: Boron; EDX: Energy dispersive X-ray; PLGA: Poly(lactic-co-glycolic acid); Zn: Zinc.***

DLS analysis

The obtained experimental data showed the presence of two granulometric intervals: [190–291] nm and [1–1.6] μm, respectively. The first interval [190–291] nm has the following structure: 14.32% of the total number of particles are of 190.2 nm, 24.05% of the total number of particles are of 207.1 nm, 27.02% of the total number are of 225 nm, 15.94% of the total number of particles are of 245.4 nm, 6.75% of 267.1 nm, and 0.81% of 290.8 nm. The second range [1–1.6] μm is organized as follows: 0.27% of the total number of particles are of 1038.7 nm, 4.86% of the total number of particles have the size of 1130.7 nm, 3.24% of the total number of particles have 1230.8 nm, 0.81% of the total number of particles have 1339.8 nm, 1.62% are at 1458.5 nm, and 0.27% at 1587.7 nm.

From the point of view of the numerical distribution, for N2 synthesis, the largest number of particles have a size around 225 nm (Figure 5A), and the particles that are the majority in the case of volume distribution (the largest volume being around the size of 1.1 μm – Figure 5B) are just a few in number.

The volume distribution also shows two granulometric ranges: [190.2–267.1] nm and [1039–1587.7] nm, respectively. The first range is presented as follows: 0.32% of the total volume are of size 190.2 nm, 0.96% of the total volume are of size 207.3 nm, 1.27% are of 225.5 nm, 9.96% are of size 245.4 nm, 0.64% are of 267.1 nm. The second interval is structured as follows: 1.91% of the total volume are of size 1.38 μm, 31.94% of the total volume are of size 1.13 μm, 28.11% of the total volume are of size 1.23 μm, 7.98% of the total volume are of size 1339 μm, 22.68% of the total volume are of size 1458 μm, 7.24% of the total volume are of 1587 μm.

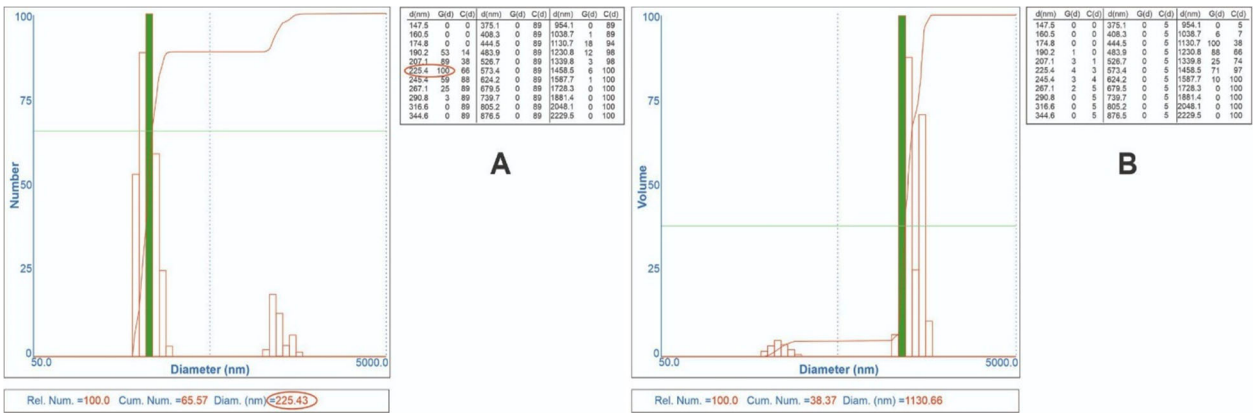

Figure 5 – ***(A) Numerical distribution of Zn–B–PLGA biocomposite particles – maximum number of particles at 225.43 nm for N2 synthesis according to experimental design model (highlighted in red); (B) Volumetric distribution of Zn–B–PLGA biocomposite particles for N2 synthesis. B: Boron; PLGA: Poly(lactic-co-glycolic acid); Zn: Zinc.***

Compared to the number distribution, in the case of the volume distribution it is found that the largest volume of particles is located in the second interval. If we analyze the numerical distribution in the second range, we find that there is a very small number of particles in this interval, but which have a large size and therefore a larger volume. Being a very small number, it is possible that they will be crowded.

PDI had values between 150–400. For example, for N2 synthesis, PDI was 0.335 and for N5 synthesis, 0.227. The lower values indicate a more monodisperse (narrow size distribution) system. Our values indicate a moderately narrow size distribution, so that in the presented conditions, we have obtained a polydisperse system but still relatively uniform [44, 45].

The ZP (-5.07±0.57 mV for n=5, Figure 6) was calculated by determining the electrophoretic mobility and applying the Henry equation.

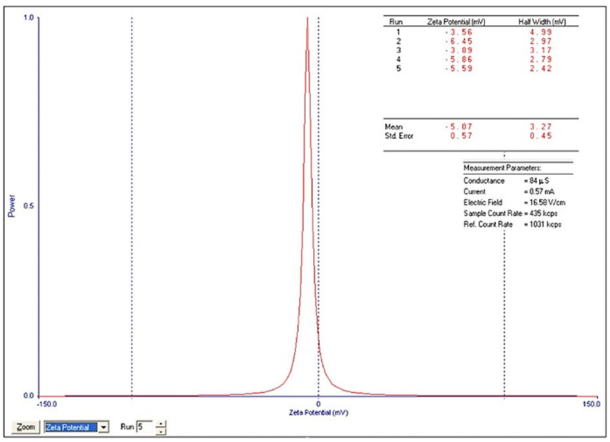

Figure 6 – ***ZP of Zn–B–PLGA biocomposite particles for N2 synthesis. B: Boron; PLGA: Poly(lactic-co-glycolic acid); Zn: Zinc; ZP: Zeta potential.***

Zn–B complex loading efficiency in Zn–B–PLGA biocomposite

LEs between 5–16% were obtained for different synthesis conditions. Figure 7 shows a typical chromatogram for N5 synthesis, with LE of 5%.

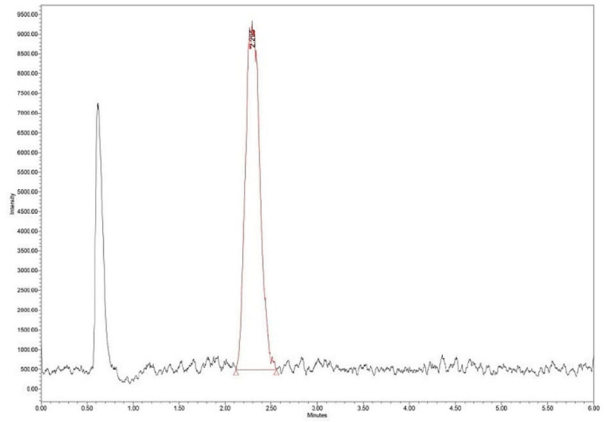

Figure 7 – ***UHPLC chromatogram for N2 synthesis of Zn–B–PLGA biocomposite according to experimental design model. B: Boron; PLGA: Poly(lactic-co-glycolic acid); UHPLC: Ultra-high performance liquid chromatography; Zn: Zinc.***

The desired LE can widely vary [46]. Through the *W/O/W* double emulsion method, incorporation efficiencies of up to 30–35% are generally obtained. This percentage may vary depending on experimental variables (PLGA/Zn–B ratio, solvent, evaporation conditions), and in the synthesis process [47]. Based on the intended therapeutic purpose and the nature of the active substance being encapsulated, there is no universally fixed minimum LE. Our future analyzes will focus on maximizing the incorporation percentage by varying the synthesis conditions.

In vitro assessment of Zn–B–PLGA biocomposite

The Vero cell line grown in the presence of Zn–B–PLGA biocomposite showed a typical fibroblast morphology, with a polygonal, elongated, and flat shape. The cell density was not significantly affected regardless of the concentrations applied as treatment. It appeared to correspond to a normal culture in the exponential growth phase. Moreover, in the positive cytotoxicity control, round cells in the process of detaching from the substrate or dying were mainly noted (Figure 8, A–I).

The viability of the treated Vero cell line was quantified using the MTT assay, considering the metabolically active viable cells. Cell morphology and density showed increased values of formazan absorbance, in the case of treatments with Zn–B–PLGA biocomposite, almost similar to those of cells grown on the genuine substrate (control). Although at higher doses there is a slight decrease in metabolic activity, the statistical analysis did not highlight significant differences compared to the negative cytotoxicity control, nor between the experimental conditions achieved. However, it can be observed that cell viability was affected above the minimum toxic concentration of 3 mM (Figure 9).

Discussions

The properties of PLGA biocomposites depend greatly on the LA/GA polymer ratio because GA has a low solubility in water while LA is extremely high soluble in water. For our synthesis, with Zn–B complex-loaded PLGA NPs as potential oral delivery system, we preferred to use PLGA with 65:35 ratio of copolymers, which is known to have a slower degradation time (2–3 months) and implicitly the release of the active principle (1–2 months) slower than PLGA 50:50 but not so great as that of PLGA 85:15 [48].

Since Zn–B complex is hydrophilic, the *W/O/W* double emulsion was successfully used, evaporating the organic solvent (DCM), which could have raised the issue of high toxicity [49].

We used PVA as a non-ionic surfactant [50] in the aqueous phase, which has hydrophilic head and a hydrophobic tail ($[CH_2CH(OH)]_n$), which is considered a critical double emulsion-stabilizing surfactant, although there are studies that consider that an increased concentration of it can affect the encapsulation efficiency [51]. Since in our previous studies of experimental design we found that the stirring speed had no major impact on efficiency or particle size, therapeutic agent encapsulation efficiency increases with concentration and pH, and decrease with PLGA concentration [52, 53], we chose to investigate how other parameters influence the size of Zn–B–PLGA biocomposite, such as

the amount of polymer added in the synthesis process and the concentration of the emulsifying agent. Our findings confirm that the size of the particles increases with increasing amounts of PLGA and PVA.

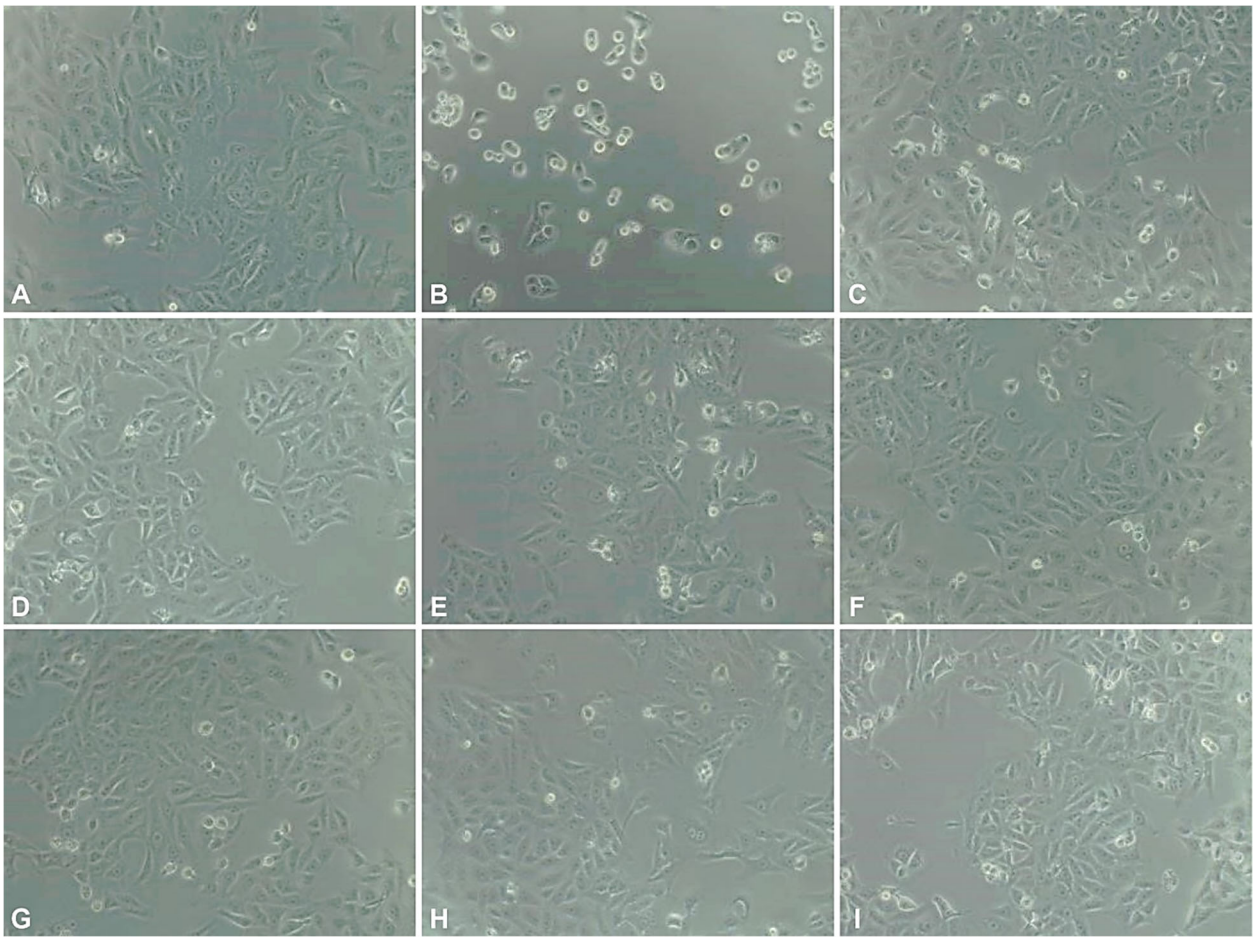

Figure 8 – ***The effect of Zn–B–PLGA biocomposite on Vero cell line morphology and density: (A) Control; (B) 5% DMSO; (C–I) The influence of Zn–B–PLGA biocomposite applied in different concentrations: 0.1 mM (C), 0.5 mM (D), 1 mM (E), 3 mM (F), 5 mM (G), 7 mM (H), and 10 mM (I), respectively. B: Boron; DMSO: Dimethyl sulfoxide; PLGA: Poly(lactic-co-glycolic acid); Zn: Zinc.***

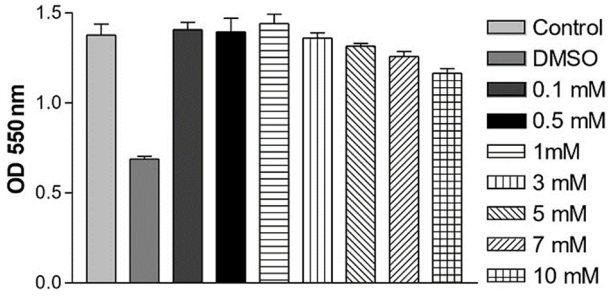

Figure 9 – ***Viability of Vero cell line treated for 24 hours with different concentrations of Zn–B–PLGA biocomposite, as determined by the MTT assay. B: Boron; DMSO: Dimethyl sulfoxide; MTT: 3-(4,5-Dimethylthiazol-2-yl)-2,5-diphenyltetrazolium bromide; OD: Optical density; PLGA: Poly(lactic-co-glycolic acid); Zn: Zinc.***

Morphology

At higher magnifications, a fibrillar interpenetrated structure can be noted with the appearance of a folded sheet. Furthermore, the SEM micrographs showed pore channels, which are characteristic to *W/O/W* double emulsion, the inner water droplets tend to come out through a diffusion process during the volatilization process of the organic solvent, as the polymer precipitates and encapsulates the active principle from W_1 aqueous phase [54]. The addition of Zn–B complex does not substantially change the morphology of the material, the active substance being most likely absorbed inside the pores, and just a smaller amount may be on the surface of the particles.

DLS measurements

PLGA is extremely safe as a drug delivery system for MPs/NPs, but NPs of any biocomposite material have specific biodistribution, with toxic effects depending on the size [55]. Even if NPs with larger sizes can incorporate a larger amount of drug, those with smaller sizes have a better penetration of biological barriers and the arrival of the drug at the site of action.

Our goal was to vary the synthesis parameters to obtain particles with dimensions of 100–200 nm, because cellular uptake is deeply affected by the size of the NPs [56]. When we obtained Zn–B–PLGA biocomposite NPs as targeted drug delivery, we also considered that the active principle loading capacity increases with size.

Zeta potential

Information regarding ZP of biopolymeric nanocomposites is very limited. The data provided by our study is novel

in this field. When immersed in water, Zn–B–PLGA biocomposite exhibits a negative ZP. The obtained negative charge is attributed to dissociation of carboxylic groups on the particle surface [57]. Also, the ZP (-5 mV) after lyophilization is not in the stability range [-25 mV; +25 mV], the literature mentions that particles with negative charges have colloid stability. Our other ZP studies on nanocomposites with PLGA showed that the centrifuged particles exhibit a much lower potential (-42 mV) compared to the lyophilized ones [58].

Biomedical applications

B, a trace element essential for human health, has recently gained attention for its potential role in modulating GM composition and function. Studies have shown that B can influence the growth and activity of specific beneficial bacteria while inhibiting the proliferation of harmful pathogens in the gut [13]. Zn is also a trace element known for its immune-modulating and anti-inflammatory properties. It also influences the composition and function of the GM [59].

PLGA is a widely used polymer in drug delivery systems for colon targeted delivery as it improves the bioavailability of many drugs to the colon [31]. Our purpose was to encapsulate the Zn–B complex within PLGA NPs to create a targeted and controlled-release delivery system for B and Zn in the intestinal tract.

PLGA NPs protect the Zn–B complex from degradation in the stomach, allowing for its targeted release in the intestinal tract, where it can have a more significant impact on the GM. The Zn–B–PLGA biocomposite is engineered to release B and Zn gradually over an extended period, ensuring a sustained and consistent supply to the gut, which is essential for microbiota health. Zn–B–PLGA biocomposite can be used in research studies to investigate the precise effects of B and Zn on GM. Additionally, the biocomposite can be developed into clinical interventions for individuals with microbiota-related health conditions [60].

Extensive research in various applications was carried out for more than a decade supporting the biocompatibility and lack of toxicity of PLGA. Mohammadi-Samani *et al.* (2015) proved the biocompatibility of PLGA microspheres for delivering peptides and proteins to the skin. It highlighted that PLGA microspheres are well-tolerated and exhibit no significant toxicity in *in vitro* and *in vivo* studies [61]. In a comprehensive review, Danhier *et al.* (2012) showed various biomedical applications of PLGA NPs, emphasizing their biocompatibility and safety [1]. Nair *et al.* (2008) explored the use of PLGA in tissue engineering. It noted that PLGA scaffolds are well-tolerated by the human body and do not induce significant toxicity, making them suitable for regenerative medicine applications [62]. The study of Guan *et al.* (2016) evaluated the *in vitro* and *in vivo* toxicity of PLGA NPs modified with polyethylene glycol (PEG). The results suggested that PEGylated PLGA NPs are safe and well-tolerated [63]. Makadia *et al.* (2011) discussed the use of PLGA as a controlled drug delivery carrier. It highlights the biodegradability and biocompatibility of PLGA, making it a safe and effective platform for sustained drug release [64].

Our research demonstrated that both Zn–B complex and Zn–B–PLGA biocomposite have lower *in vitro* toxicity levels on the Vero kidney cell line, compared to Zn orotate, the most used dietary supplement as a source of Zn [28]. Furthermore, our previous toxicodynamic studies highlighted that Zn–B complex has very low *in vivo* toxicity, being included in Category V, a practically non-toxic substance, compared to other Zn salts (orotate, chloride, oxide, sulfate) [29]. In fact, Zn–B complex can be used as stable non-toxic nutritional supplements, with enhanced rate of intestinal absorption, inducing A2M expression for healthy aging and longevity [27].

Conclusions

The Zn–B–PLGA biocomposite represents a novel delivery system for Zn and B as active principles. Its applicability will be further analyzed, and the synthesis parameters will be adjusted to better use of PLGA as novel Zn–B complex carrier. The obtained material is stable and functional, biocompatible, being able to combine the desired properties of the carrier material and the encapsulated Zn–B complex in future biomedical applications.

Conflict of interests

The authors declare that they have no conflict of interests.

Acknowledgments

This work was supported by a grant of the Ministry of Research, Innovation and Digitization, CCCDI–UEFISCDI, project number PN-III-P2-2.1-PED-2021-0804, within PNCDI III.

References

[1] Danhier F, Ansorena E, Silva JM, Coco R, Le Breton A, Préat V. PLGA-based nanoparticles: an overview of biomedical applications. J Control Release, 2012, 161(2):505–522. https://doi.org/10.1016/j.jconrel.2012.01.043 PMID: 22353619

[2] Nie H, Lee LY, Tong H, Wang CH. PLGA/chitosan composites from a combination of spray drying and supercritical fluid foaming techniques: new carriers for DNA delivery. J Control Release, 2008, 129(3):207–214. https://doi.org/10.1016/j.jconrel.2008.04.018 PMID: 18539352

[3] Anselmo AC, Mitragotri S. An overview of clinical and commercial impact of drug delivery systems. J Control Release, 2014, 190:15–28. https://doi.org/10.1016/j.jconrel.2014.03.053 PMID: 24747160 PMCID: PMC4142089

[4] Molavi F, Barzegar-Jalali M, Hamishehkar H. Polyester based polymeric nano and microparticles for pharmaceutical purposes: a review on formulation approaches. J Control Release, 2020, 320:265–282. https://doi.org/10.1016/j.jconrel.2020.01.028 PMID: 31962095

[5] Zhong H, Chan G, Hu Y, Hu H, Ouyang D. A comprehensive map of FDA-approved pharmaceutical products. Pharmaceutics, 2018, 10(4):263. https://doi.org/10.3390/pharmaceutics10040263 PMID: 30563197 PMCID: PMC6321070

[6] Wan B, Bao Q, Burgess D. Long-acting PLGA microspheres: advances in excipient and product analysis toward improved product understanding. Adv Drug Deliv Rev, 2023, 198:114857. https://doi.org/10.1016/j.addr.2023.114857 PMID: 37149041

[7] Andhariya JV, Jog R, Shen J, Choi S, Wang Y, Zou Y, Burgess DJ. *In vitro–in vivo* correlation of parenteral PLGA microspheres: effect of variable burst release. J Control Release, 2019, 314:25–37. https://doi.org/10.1016/j.jconrel.2019.10.014 PMID: 31654687

[8] Miao Y, Cui H, Dong Z, Ouyang Y, Li Y, Huang Q, Wang Z. Structural evolution of polyglycolide and poly(glycolide-*co*-lactide) fibers during *in vitro* degradation with different heat-setting temperatures. ACS Omega, 2021, 6(43):29254–29266. https://doi.org/10.1021/acsomega.1c04974 PMID: 34746613 PMCID: PMC8567347

[9] Proikakis CS, Tarantili PA, Andreopoulos AG. The role of polymer/drug interactions on the sustained release from poly (DL-lactic acid) tablets. Eur Polym J, 2006, 42(12):3269–3276. https://doi.org/10.1016/j.eurpolymj.2006.08.023 https://www.sciencedirect.com/science/article/abs/pii/S0014305706002953?via%3Dihub

[10] Kim HJ, Furukawa Y, Kakegawa T, Bita A, Scorei R, Benner SA. Evaporite borate-containing mineral ensembles make phosphate available and regiospecifically phosphorylate ribonucleosides: borate as a multifaceted problem solver in prebiotic chemistry. Angew Chem Int Ed Engl, 2016, 55(51):15816–15820. https://doi.org/10.1002/anie.201608001 PMID: 27862722

[11] Uluisik I, Karakaya HC, Koc A. The importance of boron in biological systems. J Trace Elem Med Biol, 2018, 45:156–162. https://doi.org/10.1016/j.jtemb.2017.10.008 PMID: 29173473

[12] Mitruţ I, Cojocaru MO, Scorei IR, Biţă A, Mogoşanu GD, Popescu M, Olimid DA, Manolea HO. Preclinical and histological study of boron-containing compounds hydrogels on experimental model of periodontal disease. Rom J Morphol Embryol, 2021, 62(1):219–226. https://doi.org/10.47162/RJME.62.1.21 PMID: 34609424 PMCID: PMC8597384

[13] Biţă A, Scorei IR, Bălşeanu TA, Ciocîlteu MV, Bejenaru C, Radu A, Bejenaru LE, Rău G, Mogoşanu GD, Neamţu J, Benner SA. New insights into boron essentiality in humans and animals. Int J Mol Sci, 2022, 23(16):9147. https://doi.org/10.3390/ijms23169147 PMID: 36012416 PMCID: PMC9409115

[14] Karatekeli S, Demirel HH, Zemheri-Navruz F, Ince S. Boron exhibits hepatoprotective effect together with antioxidant, anti-inflammatory, and anti-apoptotic pathways in rats exposed to aflatoxin B_1. J Trace Elem Med Biol, 2023, 77:127127. https://doi.org/10.1016/j.jtemb.2023.127127 PMID: 36641954

[15] Arciniega-Martínez IM, Romero-Aguilar KS, Farfán-García ED, García-Machorro J, Reséndiz-Albor AA, Soriano-Ursúa MA. Diversity of effects induced by boron-containing compounds on immune response cells and on antibodies in basal state. J Trace Elem Med Biol, 2022, 69:126901. https://doi.org/10.1016/j.jtemb.2021.126901 PMID: 34801850

[16] Biţă A, Scorei IR, Rangavajla N, Bejenaru LE, Rău G, Bejenaru C, Ciocîlteu MV, Dincă L, Neamţu J, Bunaciu A, Rogoveanu OC, Pop MI, Mogoşanu GD. Diester chlorogeno-borate complex: a new naturally occurring boron-containing compound. Inorganics, 2023, 11(3):112. https://doi.org/10.3390/inorganics11030112 https://www.mdpi.com/2304-6740/11/3/112

[17] Mitruţ I, Scorei IR, Manolea HO, Biţă A, Mogoantă L, Neamţu J, Bejenaru LE, Ciocîlteu MV, Bejenaru C, Rău G, Mogoşanu GD. Boron-containing compounds in Dentistry: a narrative review. Rom J Morphol Embryol, 2022, 63(3):477–483. https://doi.org/10.47162/RJME.63.3.01 PMID: 36588485 PMCID: PMC9926150

[18] Scorei IR, Ciocilteu MV, Bita A, Rau G, Mogosanu GD, Dinca L. Zinc–Boron–PLGA biocomposite-based materials and uses thereof. United States Patent and Trademark Office (USPTO), Provisional Patent Application No. 63536442, September 4, 2023. https://www.uspto.gov/patents/basics/types-patent-applications/provisional-application-patent

[19] Donoiu I, Militaru C, Obleagă O, Hunter JM, Neamţu J, Biţă A, Scorei IR, Rogoveanu OC. Effects of boron-containing compounds on cardiovascular disease risk factors – a review. J Trace Elem Med Biol, 2018, 50:47–56. https://doi.org/10.1016/j.jtemb.2018.06.003 PMID: 30262316

[20] Hunter DJ, March L, Chew M. Osteoarthritis in 2020 and beyond: a Lancet Commission. Lancet, 2020, 396(10264):1711–1712. https://doi.org/10.1016/S0140-6736(20)32230-3 PMID: 33159851

[21] Prasad AS. Chapter 20 – Discovery of zinc for human health and biomarkers of zinc deficiency. In: Collins JF (ed). Molecular, genetic, and nutritional aspects of major and trace minerals. Academic Press–Elsevier, London, UK, 2017, 241–260. https://doi.org/10.1016/B978-0-12-802168-2.00020-8 https://www.sciencedirect.com/science/article/pii/B9780128021682000208?via%3Dihub

[22] Stefanidou M, Maravelias C, Dona A, Spiliopoulou C. Zinc: a multipurpose trace element. Arch Toxicol, 2006, 80(1):1–9. https://doi.org/10.1007/s00204-005-0009-5 PMID: 16187101

[23] McCall KA, Huang C, Fierke CA. Function and mechanism of zinc metalloenzymes. J Nutr, 2000, 130(5S Suppl):1437S–1446S. https://doi.org/10.1093/jn/130.5.1437S PMID: 10801957

[24] Scarpellini E, Balsiger LM, Maurizi V, Rinninella E, Gasbarrini A, Giostra N, Santori P, Abenavoli L, Rasetti C. Zinc and gut microbiota in health and gastrointestinal disease under the COVID-19 suggestion. Biofactors, 2022, 48(2):294–306. https://doi.org/10.1002/biof.1829 PMID: 35218585 PMCID: PMC9082519

[25] Wu C, Labrie J, Tremblay YD, Haine D, Mourez M, Jacques M. Zinc as an agent for the prevention of biofilm formation by pathogenic bacteria. J Appl Microbiol, 2013, 115(1):30–40. https://doi.org/10.1111/jam.12197 PMID: 23509865

[26] de Queiroz CAA, Fonseca SGC, Frota PB, Figueiredo IL, Aragão KS, Magalhães CEC, de Carvalho CBM, Lima AÂM, Ribeiro RA, Guerrant RL, Moore SR, Oriá RB. Zinc treatment ameliorates diarrhea and intestinal inflammation in undernourished rats. BMC Gastroenterol, 2014, 14:136. https://doi.org/10.1186/1471-230X-14-136 PMID: 25095704 PMCID: PMC4142448

[27] Biţă A, Scorei IR, Bălşeanu TA, Rău G, Ciocîlteu MV, Mogoşanu GD. Zinc–boron complex-based dietary supplements for longevity and healthy life. Curr Health Sci J, 2023, 49(3):381–387. https://doi.org/10.12865/CHSJ.49.03.10 https://www.chsjournal.org/article/49/3/10/

[28] Oancea CN, Cîmpean A, Ion R, Neamţu J, Biţă A, Scorei IR, Neamţu AS, Rogoveanu OC, Zaharie SI, Birkenmeier G. *In vitro* cytotoxicity of zinc fructoborate, a novel zinc–boron active natural complex. Curr Health Sci J, 2018, 44(2):113–117. https://doi.org/10.12865/CHSJ.44.02.03 PMID: 30746157 PMCID: PMC6320461

[29] Scorei IR. Novel active zinc and boron-based dietary supplements for longevity and healthy life. Grant of the Romanian National Authority for Scientific Research and Innovation, CNCS/CCCDI–UEFISCDI, Project No. PN-III-P2-2.1-PED-2016-0410, 2017. https://www.naturalresearch.ro/projects/#

[30] Hunter JM, Nemzer BV, Rangavajla N, Biţă A, Rogoveanu OC, Neamţu J, Scorei IR, Bejenaru LE, Rău G, Bejenaru C, Mogoşanu GD. The fructoborates: part of a family of naturally occurring sugar-borate complexes – biochemistry, physiology, and impact on human health: a review. Biol Trace Elem Res, 2019, 188(1):11–25. https://doi.org/10.1007/s12011-018-1550-4 PMID: 30343480 PMCID: PMC6373344

[31] Lozoya-Agullo I, Araújo F, González-Álvarez I, Merino-Sanjuán M, González-Álvarez M, Bermejo M, Sarmento B. PLGA nanoparticles are effective to control the colonic release and absorption on ibuprofen. Eur J Pharm Sci, 2018, 115:119–125. https://doi.org/10.1016/j.ejps.2017.12.009 PMID: 29248559

[32] Naeem M, Bae J, Oshi MA, Kim MS, Moon HR, Lee BL, Im E, Jung Y, Yoo JW. Colon-targeted delivery of Cyclosporine A using dual-functional Eudragit® FS30D/PLGA nanoparticles ameliorates murine experimental colitis. Int J Nanomedicine, 2018, 13:1225–1240. https://doi.org/10.2147/IJN.S157566 PMID: 29535519 PMCID: PMC5836652

[33] Scorei IR. Calcium fructoborate: plant-based dietary boron as potential medicine for cancer therapy. Front Biosci (Schol Ed), 2011, 3(1):205–215. https://doi.org/10.2741/s145 PMID: 21196370

[34] Hunter JM. Compositions and methods for borocarbohydrate complexes. United States Patent and Trademark Office (USPTO), Patent No. 9102700 B1, August 11, 2015. https://patents.google.com/patent/US9102700

[35] Hubbard SA. Comparative toxicology of borates. Biol Trace Elem Res, 1998, 66(1–3):343–357. https://doi.org/10.1007/BF02783147 PMID: 10050929

[36] Korolenko SE, Avdeeva VV, Malinina EA, Kuznetsov NT. Zinc(II) and cadmium(II) coordination compounds with boron cluster anions: classification of compounds depending on strength of metal–boron cage interaction and analysis of structures (review). Russ J Inorg Chem, 2021, 66(9):1350–1373. https://doi.org/10.1134/S0036023621090047 https://link.springer.com/article/10.1134/S0036023621090047

[37] Liao TT, Shi YL, Jia JW, Jia RW, Wang L. Sensitivity of morphological change of Vero cells exposed to lipophilic compounds and its mechanism. J Hazard Mater, 2010, 179(1–3):1055–1064. https://doi.org/10.1016/j.jhazmat.2010.03.113 PMID: 20427127

[38] Berridge MV, Herst PM, Tan AS. Tetrazolium dyes as tools in cell biology: new insights into their cellular reduction. Biotechnol Annu Rev, 2005, 11:127–152. https://doi.org/10.1016/S1387-2656(05)11004-7 PMID: 16216776

[39] Kamaly N, Yameen B, Wu J, Farokhzad OC. Degradable controlled-release polymers and polymeric nanoparticles: mechanisms of controlling drug release. Chem Rev, 2016, 116(4):2602–2663. https://doi.org/10.1021/acs.chemrev.5b00346 PMID: 26854975 PMCID: PMC5509216

[40] Silva ATCR, Cardoso BCO, Silva MESR, Freitas RFS, Sousa RG. Synthesis, characterization, and study of PLGA copolymer *in vitro* degradation. J Biomater Nanobiotechnol, 2015, 6:8–19. https://doi.org/10.4236/jbnb.2015.61002 https://www.scirp.org/journal/paperinformation?paperid=52929

[41] Ciocîlteu MV, Podgoreanu P, Delcaru C, Chifiriuc MC, Manda CV, Biţă A, Popescu M, Amzoiu E, Croitoru O, Bleotu C, Bostan M, Neamţu J. PLGA–Gentamicin biocomposite materials with potential antimicrobial applications in orthopedics. Farmacia 2019, 67(4):580–586. https://doi.org/10.31925/farmacia.2019.4.4 https://farmaciajournal.com/issue-articles/plga-gentamicin-biocomposite-materials-with-potential-antimicrobial-applications-in-orthopedics/
[42] Huang W, Zhang C. Tuning the size of poly(lactic-*co*-glycolic acid) (PLGA) nanoparticles fabricated by nanoprecipitation. Biotechnol J, 2018, 13(1):1700203. https://doi.org/10.1002/biot.201700203 PMID: 28941234 PMCID: PMC5924600
[43] Prakapenka AV, Bimonte-Nelson HA, Sirianni RW. Engineering poly(lactic-*co*-glycolic acid) (PLGA) micro- and nano-carriers for controlled delivery of 17*β*-estradiol. Ann Biomed Eng, 2017, 45(7):1697–1709. https://doi.org/10.1007/s10439-017-1859-8 PMID: 28634732 PMCID: PMC5599155
[44] Mostafa MM, Amin MM, Zakaria MY, Hussein MA, Shamaa MM, Abd El-Halim SM. Chitosan surface-modified PLGA nanoparticles loaded with cranberry powder extract as a potential oral delivery platform for targeting colon cancer cells. Pharmaceutics, 2023, 15(2):606. https://doi.org/10.3390/pharmaceutics15020606 PMID: 36839928 PMCID: PMC9964659
[45] Wang J, Wang F, Li X, Zhou Y, Wang H, Zhang Y. Uniform carboxymethyl chitosan-enveloped Pluronic F68/poly(lactic-*co*-glycolic acid) nano-vehicles for facilitated oral delivery of Gefitinib, a poorly soluble antitumor compound. Colloids Surf B Biointerfaces, 2019, 177:425–432. https://doi.org/10.1016/j.colsurfb.2019.02.028 PMID: 30798063
[46] Sun SB, Liu P, Shao FM, Miao QL. Formulation and evaluation of PLGA nanoparticles loaded Capecitabine for prostate cancer. Int J Clin Exp Med, 2015, 8(10):19670–19681. PMID: 26770631 PMCID: PMC4694531
[47] Huang WF, Tsui GCP, Tang CY, Yang M. Optimization strategy for encapsulation efficiency and size of drug loaded silica xerogel/polymer core–shell composite nanoparticles prepared by gelation–emulsion method. Polym Eng Sci, 2018, 58(5):742–751. https://doi.org/10.1002/pen.24609 https://4spepublications.onlinelibrary.wiley.com/doi/abs/10.1002/pen.24609
[48] Houchin ML, Topp EM. Physical properties of PLGA films during polymer degradation. J Appl Polym Sci, 2009, 114(5):2848–2854. https://doi.org/10.1002/app.30813 https://onlinelibrary.wiley.com/doi/abs/10.1002/app.30813
[49] Kluin OS, van der Mei HC, Busscher HJ, Neut D. Biodegradable *vs* non-biodegradable antibiotic delivery devices in the treatment of osteomyelitis. Expert Opin Drug Deliv, 2013, 10(3):341–351. https://doi.org/10.1517/17425247.2013.751371 PMID: 23289645
[50] Hariharan S, Bhardwaj V, Bala I, Sitterberg J, Bakowsky U, Ravi Kumar MN. Design of estradiol loaded PLGA nanoparticulate formulations: a potential oral delivery system for hormone therapy. Pharm Res, 2006, 23(1):184–195. https://doi.org/10.1007/s11095-005-8418-y PMID: 16267632
[51] Arriaga LR, Datta SS, Kim SH, Amstad E, Kodger TE, Monroy F, Weitz DA. Ultrathin shell double emulsion templated giant unilamellar lipid vesicles with controlled microdomain formation. Small, 2014, 10(5):950–956. https://doi.org/10.1002/smll.201301904 PMID: 24150883
[52] Turcu-Ştiolică A, Ciocîlteu MV, Podgoreanu P, Neacşu I, Ionescu (Filip) OL, Nicolicescu C, Neamţu J, Amzoiu E, Amzoiu E, Manda CV. PLGA–Gentamicin and PLGA–Hydroxyapatite–Gentamicin microspheres for medical applications. Pharm Chem J, 2022, 56(5):645–653. https://doi.org/10.1007/s11094-022-02689-w https://link.springer.com/article/10.1007/s11094-022-02689-w
[53] Ciocilteu MV, Nicolaescu OE, Mocanu AG, Nicolicescu C, Rau G, Neamtu J, Amzoiu E, Amzoiu E, Oancea C, Turcu-Stiolica A. Process optimization using quality by design (QBD) approach of a Gentamicin loaded PLGA biocomposite. J Sci Arts, 2021, 57(4):1069–1080. https://doi.org/10.46939/J.Sci.Arts-21.4-b02 https://www.josa.ro/index.html?https%3A//www.josa.ro/josa.html
[54] Mezzenga R, Folmer BM, Hughes E. Design of double emulsions by osmotic pressure tailoring. Langmuir, 2004, 20(9):3574–3582. https://doi.org/10.1021/la036396k PMID: 15875386
[55] Berchane NS, Carson KH, Rice-Ficht AC, Andrews MJ. Effect of mean diameter and polydispersity of PLG microspheres on drug release: experiment and theory. Int J Pharm, 2007, 337(1–2):118–126. https://doi.org/10.1016/j.ijpharm.2006.12.037 PMID: 17289316
[56] He C, Hu Y, Yin L, Tang C, Yin C. Effects of particle size and surface charge on cellular uptake and biodistribution of polymeric nanoparticles. Biomaterials, 2010, 31(13):3657–3666. https://doi.org/10.1016/j.biomaterials.2010.01.065 PMID: 20138662
[57] Kadri R, Elkhoury K, Ben Messaoud G, Kahn C, Tamayol A, Mano JF, Arab-Tehrany E, Sánchez-González L. Physico-chemical interactions in nanofunctionalized alginate/GelMA IPN hydrogels. Nanomaterials (Basel), 2021, 11(9):2256. https://doi.org/10.3390/nano11092256 PMID: 34578572 PMCID: PMC8465058
[58] Postelnicu RA, Ciocîlteu MV, Neacşu IA, Nicolicescu C, Costachi A, Amzoiu M, Neamţu J, Pisoschi CG, Mocanu AG, Rău G, Amzoiu E. PLGA–Bisphosphonates conjugated nanoparticles: synthesis and morphological characterization. Farmacia, 2023, 71(1):83–90. https://doi.org/10.31925/farmacia.2023.1.11 https://farmaciajournal.com/issue-articles/plga-bisphosphonates-conjugated-nanoparticles-synthesis-and-morphological-characterization/
[59] Pajarillo EAB, Lee E, Kang DK. Trace metals and animal health: interplay of the gut microbiota with iron, manganese, zinc, and copper. Anim Nutr, 2021, 7(3):750–761. https://doi.org/10.1016/j.aninu.2021.03.005 PMID: 34466679 PMCID: PMC8379138
[60] Hua S, Marks E, Schneider JJ, Keely S. Advances in oral nano-delivery systems for colon targeted drug delivery in inflammatory bowel disease: selective targeting to diseased *versus* healthy tissue. Nanomedicine, 2015, 11(5):1117–1132. https://doi.org/10.1016/j.nano.2015.02.018 PMID: 25784453
[61] Mohammadi-Samani S, Taghipour B. PLGA micro and nanoparticles in delivery of peptides and proteins; problems and approaches. Pharm Dev Technol, 2015, 20(4):385–393. https://doi.org/10.3109/10837450.2014.882940 PMID: 24483777
[62] Nair LS, Laurencin CT. Biodegradable polymers as biomaterials. Prog Polym Sci, 2007, 32(8–9):762–798. https://doi.org/10.1016/j.progpolymsci.2007.05.017 https://www.sciencedirect.com/science/article/abs/pii/S0079670007000664?via%3Dihub
[63] Guan Q, Sun S, Li X, Lv S, Xu T, Sun J, Feng W, Zhang L, Li Y. Preparation, *in vitro* and *in vivo* evaluation of mPEG–PLGA nanoparticles co-loaded with Syringopicroside and Hydroxytyrosol. J Mater Sci Mater Med, 2016, 27(2):24. https://doi.org/10.1007/s10856-015-5641-x PMID: 26704541
[64] Makadia HK, Siegel SJ. Poly lactic-*co*-glycolic acid (PLGA) as biodegradable controlled drug delivery carrier. Polymers (Basel), 2011, 3(3):1377–1397. https://doi.org/10.3390/polym3031377 PMID: 22577513 PMCID: PMC3347861

Corresponding authors

Ion Romulus Scorei, Professor, PhD, Department of Biochemistry, BioBoron Research Institute, S.C. Natural Research S.R.L., 31B Dunării Street, 207465 Podari, Dolj County, Romania; Phone +40351–407 543, e-mail: romulus_ion@yahoo.com

Claudiu Nicolicescu, Associate Professor, PhD, Department of Engineering and Management of Technological Systems, Faculty of Mechanics, University of Craiova, 1 Călugăreni Street, 220037 Drobeta Turnu-Severin, Mehedinţi County, Romania; Phone +40252–333 431, e-mail: nicolicescu_claudiu@yahoo.com

Received: December 15, 2023 *Accepted: December 30, 2023*